JACC: CARDIOVASCULAR IMAGING VOL. ■, NO. ■, 2020

CLINICAL RESEARCH

Diabetic Cardiomiopathy Progression is Triggered by miR122-5p and Involves Extracellular Matrix

A 5-Year Prospective Study

Riccardo Pofi, MD,[a,*] Elisa Giannetta, MD, PhD,[a,*] Nicola Galea, MD,[a] Marco Francone, MD, PhD,[b] Federica Campolo, PhD,[a] Federica Barbagallo, PhD,[a] Daniele Gianfrilli, MD, PhD,[a] Mary Anna Venneri, PhD,[a] Tiziana Filardi, MD,[a] Cristiano Cristini, MD, PhD,[c] Gabriele Antonini, MD, PhD,[c] Roberto Badagliacca, MD, PhD,[d] Giacomo Frati, MD, PhD,[e,f] Andrea Lenzi, MD, PhD,[a] Iacopo Carbone, MD, PhD,[b] Andrea M. Isidori, MD, PhD[a]

ABSTRACT

OBJECTIVES The purpose of this study was to follow the long-term progression of diabetic cardiomyopathy by combining cardiac magnetic resonance (CMR) and molecular analysis.

BACKGROUND The evolution of diabetic cardiomyopathy to heart failure affects patients'morbidity and mortality. CMR is the gold standard to assess cardiac remodeling, but there is a lack of markers linked to the mechanism of diabetic cardiomyopathy progression.

METHODS Five-year longitudinal study on patients with type 2 diabetes mellitus (T2DM) enrolled in the Cardiovascular Effects of Chronic Sildenafil in Men With Type 2 Diabetes (CECSID) trial (NCT00692237) compared with nondiabetic age-matched controls. CMR with tagging together with metabolic and molecular assessments were performed at baseline and 5-year follow-up.

RESULTS Seventy-nine men (age 64 ± 8 years) enrolled, comprising 59 men with T2DM compared with 20 nondiabetic age-matched controls. Longitudinal CMR with tagging showed an increase in ventricular mass (ΔLVMi = 13.47 ± 29.66 g/m^2; p = 0.014) and a borderline increase in end-diastolic volume (ΔEDVi = 5.16 ± 14.71 ml/m^2; p = 0.056) in men with T2DM. Cardiac strain worsened ($\Delta\sigma$ = 1.52 ± 3.85%; p = 0.033) whereas torsion was unchanged ($\Delta\theta$ = 0.24 ± 4.04°; p = 0.737), revealing a loss of the adaptive equilibrium between strain and torsion. Contraction dynamics showed a decrease in the systolic time-to-peak (ΔTtP = −35.18 ± 28.81 ms; p < 0.001) and diastolic early recoil-rate (ΔRR = −20.01 ± 19.07 s^{-1}; p < 0.001). The ejection fraction and metabolic parameters were unchanged. Circulating miR microarray revealed an up-regulation of miR122-5p. Network analysis predicted the matrix metalloproteinases (MMPs) MMP-16 and MMP-2 and their regulator (tissue inhibitors of metalloproteinases) as targets. In db/db mice we demonstrated that miR122-5p expression is associated with diabetic cardiomyopathy, that in the diabetic heart is overexpressed, and that, in vitro, it regulates MMP-2. Finally, we demonstrated that miR122-5p overexpression affects the extracellular matrix through MMP-2 modulation.

CONCLUSIONS Within 5 years of diabetic cardiomyopathy onset, increasing cardiac hypertrophy is associated with progressive impairment in strain, depletion of the compensatory role of torsion, and changes in viscoelastic contraction dynamics. These changes are independent of glycemic control and paralleled by the up-regulation of specific microRNAs targeting the extracellular matrix (Cardiovascular Effects of Chronic Sildenafil in Men With Type 2 Diabetes [CECSID]; NCT00692237) (J Am Coll Cardiol Img 2020;■:■–■) © 2020 The Authors. Published by Elsevier on behalf of the American College of Cardiology Foundation. This is an open access article under the CC BY-NC-ND license (http://creativecommons.org/licenses/by-nc-nd/4.0/).

ISSN 1936-878X https://doi.org/10.1016/j.jcmg.2020.10.009

ABBREVIATIONS AND ACRONYMS

CMR = cardiac magnetic resonance

ECM = extracellular matrix

EDVi = indexed end-diastolic volume

EF = ejection fraction

HF = heart failure

HfpEF = heart failure with preserved ejection fraction

HfrEF = heart failure with reduced ejection fraction

LGE = late gadolinium enhancement

LV = left ventricle

LVMi = indexed left ventricular mass

miRNA = microRNA

MMP = matrix metalloproteinase

mRNA = messenger RNA

qPCR = quantitative polymerase chain reaction

RR = recoil rate

TtP = time to peak

T2DM = type 2 diabetes mellitus

Cardiovascular complications are the main causes of morbidity and mortality in patients with type 2 diabetes mellitus (T2DM), accounting for about two thirds of overall deaths (1). The Framingham Heart Study showed a 2- to 5-fold increase in heart failure (HF) in individuals with T2DM, even when adjusted for the most common risk factors (2), supporting the existence of a specific diabetic cardiomyopathy.

Traditionally, diabetic cardiomyopathy was described as an early diastolic dysfunction triggered by hyperglycemia or inflammatory myocardial injuries, which can occur in the absence of other known cardiovascular diseases, potentially evolving into a systolic dysfunction (3). Recently, the initial stage was recorded according to the common categories for HF as a restrictive pattern with preserved ejection fraction (HFpEF), which can evolve toward dilated with reduced ejection fraction (HFrEF) (4).

In the 2012 Cardiovascular Effects of Chronic Sildenafil in Men With Type 2 Diabetes (CECSID) trial, we demonstrated that cardiac magnetic resonance (CMR) with tagging accurately identifies the early asymptomatic stages of diabetic cardiomyopathy. We validated the use of CMR in short-term follow-up and described a decoupling between the shortening of cardiac fibers (strain), which was reduced, and the rotational motion of the apex relative to the base (torsion), which was increased (5).

Despite the increasing awareness of cardiac risk in diabetic cardiomyopathy, few studies have investigated the role of glycemic control for its evolution, but all seem to concur that strict glycemic control does not halt or reverse cardiac disease progression (6). Thus, there is an urgent need for biomarkers to monitor cardiac worsening. MicroRNAs (miRNAs) have recently emerged as potential noninvasive biomarkers offering diagnostic, prognostic, and therapeutic targets for diabetic cardiomyopathy (7). However, few studies validated their role prospectively and provided a biologic proof for the mechanism involved in the clinical settings they were identified.

To investigate the long-term progression of cardiac remodeling in T2DM and identify possible clinically useful markers, we followed up all patients enrolled in the CECSID trial annually and repeated CMR-tagged imaging after 5 years. We performed a microarray to identify the mi-RNAs differently expressed with diabetic cardiomyopathy progression. We tested their activity in vivo using a diabetic mouse model and in vitro using various cell cultures exposed to high glucose. Among more than 3,000 tested miRNAs, we found that the miR-122-5p, previously demonstrated to play a role in the pathogenesis of microvascular cardiac diseases (8,9), was significantly associated with diabetic cardiomyopathy. Then, we proved, for the first time, that miR-122-5p targets the metalloproteinases and cardiac extracellular matrix (ECM), providing a molecular explanation for the observed changes in the contraction dynamics of the diabetic heart.

METHODS

SUBJECTS AND PROTOCOL. Patients with T2DM participating in the CECSID trial (NCT00692237) were followed up yearly (from 2008 to 2012) with a routine clinical assessment (Methods 3 in Supplemental Appendix) and a full CMR imaging evaluation performed 5 years after the first imaging. The inclusion and exclusion criteria were previously described (5). Twenty nondiabetic age-matched men were recruited from our outpatient clinic (for nonfunctioning thyroid nodules) and enrolled as controls for the follow-up assessment. The CMR scan evaluated cardiac contraction (strain and torsion), geometry (indexed left ventricular mass [LVMi] and end-diastolic volume [EDVi]), dynamics (as clarified later in this paper), performance (ejection fraction [EF]), and areas of myocardial fibrosis (late gadolinium enhancement [LGE]).

From the [a]Department of Experimental Medicine, "Sapienza" University of Rome, Rome, Italy; [b]Department of Radiological, Oncological and Pathological Sciences, "Sapienza" University of Rome, Rome, Italy; [c]Department of Obstetrical and Gynaecological Sciences and Urological Sciences, "Sapienza" University of Rome, Rome, Italy; [d]Department of Cardiovascular and Respiratory Diseases, "Sapienza" University of Rome, Rome, Italy; [e]Department of Medico-Surgical Sciences and Biotechnologies, Sapienza University of Rome, Latina, Italy; and the [f]Istituti di Ricovero e Cura a Carattere Scientifico (IRCCS) NEUROMED, Pozzilli, Italy. *Drs. Pofi and Giannetta contributed equally to this work.

The authors attest they are in compliance with human studies committees and animal welfare regulations of the authors' institutions and Food and Drug Administration guidelines, including patient consent where appropriate. For more information, visit the *JACC: Cardiovascular Imaging* author instructions page.

Manuscript received August 10, 2020; revised manuscript received October 14, 2020, accepted October 15, 2020.

Alongside clinical and radiological evaluations (CMR), circulating plasma miRNAs were collected at enrollment and 5-year follow-up. A microarray analysis with more than 3,000 known human miRNAs was undertaken to identify those differentially expressed. The identified miRNAs were tested against diabetic cardiomyopathy progression. The potential biologic targets for the identified miRNAs were screened using web-based software. Then ex vivo (diabetic mouse models) and in vitro experiments (miRNA Transfection, Luciferase assay, and zymography) were carried out to provide direct proof of their direct involvement in the molecular pathways sustaining diabetic cardiomyopathy progression. All subjects gave their written informed consent. The clinical protocol was approved by the Hospital Ethics Committee (746/07).

CMR IMAGING. CMR imaging studies were performed by an experienced operator (NG) as previously described (5) (Methods 4 in Supplemental Appendix) using a 1.5-T scanner (Avanto, Siemens, Healthcare Solutions, Erlangen, Germany) with an 8-element phased-array surface receiver coil and electrocardiogram triggering. Ventricular volumes were measured using breath-hold balanced, steady-state free precession sequences (cineMR) of 10 to 12 short-axis slices covering the whole left ventricle (LV) from base to apex. Myocardial strain and torsion were calculated applying on cineMR sequences a grid generated by saturating orthogonal tags. LGE imaging was performed after the intravenous injection of contrast agent (0.1 mmol/kg Gd-DOTA, Guerbet, Villepinte, France) to rule out previous myocardial infarction. All sequences were performed in vertical and horizontal long- and short-axis orientations.

Kinetics, geometry, and cardiac performance were analyzed using Harmonic Phase tecnology (HARP, version 1.1, Diagnosoft Inc., Morrisville, North Carolina) (Methods 4 in Supplemental Appendix) and revealed a low intraobserver variability.

CMR CARDIAC CONTRACTION DYNAMICS. Using nonlinear regression analysis with dynamic fit, we previously (5) showed that the best equation describing systolic twist is a monoexponential rise to a nonzero asymptote (Methods 4 in Supplemental Appendix), $T_t(t) = T_{max}[1-\exp(b_t \cdot t)]$, where $T_t(t)$ is the instantaneous LV torsion function of time t, T_{max} is the asymptotic maximum torsion, and b_t is the twist time constant. Conversely, diastolic untwist is best described by a monoexponential decay (with a zero-torsion asymptote) as $T_{ut}(t) = T_o\exp(-b_{ut} \cdot t)$, where $T_{ut}(t)$ is the instantaneous LV recoil, T_o is the proto-diastolic torsion before the onset of torsion decay and b_{ut} is the untwist (or recoil) time constant; b_{ut} can be used as an index for LV relaxation.

Although this is an oversimplified model, the equation supports the hypothesis that the CMR parameters describing LV torsion are directly related to contraction and the viscoelasticity of the myocardium.

Additional calculated parameters were the time to peak (TtP), defined as the time (ms) the heart takes to reach T_{max}; and the normalized recoil rate (RR) = $d(T_{ut})/dt$, defined as the slope of the linear regression of recoil during the first 100 ms after peak torsion. Calculated in this way, the RR was then normalized for peak torsion as $RR = RR/T_{max.}$

For clinical interpretation of dynamics see Methods 2 in Supplemental Appendix.

IDENTIFICATION OF DIFFERENTIALLY EXPRESSED miRNAs. The longitudinal analysis of serum miRNA profiles was assessed at baseline and at 5 years of follow-up using a double approach (Methods 5 to 8 in Supplemental Appendix). The entire set was randomly split into two. Half the samples were processed using an array strategy and the other one-half were used to confirm the findings by real time quantitative polymerase chain reaction (RT-qPCR). Array data in patients with T2DM were also further tested against a different control group of nondiabetic subjects with pulmonary hypertension to exclude miRNA modulation related to nondiabetes-specific cardiovascular disorders (data not shown).

DIABETIC MOUSE MODEL. Male BKS.Cg-Dock7m+/+LeprdbJ (db/db) mice aged 5 and 22 weeks (6 in each group), obtained from the Charles River Laboratory (Calco, Italy), were maintained in a pathogen-free facility. All experiments were performed in accordance with Italian and European law (2010/63/EU) and the study was approved by the Sapienza University's Animal Research Ethics Committee and by the Italian Ministry of Health (165/2016-PR). Fasting blood glucose was determined in each group at 5 and 10 weeks of age, respectively. db/db mice are widely used to follow T2DM progression and compliances because they present hyperinsulinemia early and develop severe T2DM by 8 to 10 weeks of age (10,11). The 5-week-old mice were thus considered as normoglycemic, hyperinsulinemic controls compared with the diabetic older mice exhibiting features of diabetic cardiomyopathy.

CELL CULTURES IN LOW AND HIGH GLUCOSE. HEK293 and HL-1 cell culture were cultured as previously described (12). Human corpus cavernosum primary cultures (human pericytes) were obtained from nondiabetic donors undergoing penile

TABLE 1 Characteristics of the 51 Patients With T2DM Completing Both the Baseline and 5-Year Follow-Up CMR Assessment and 20 Nondiabetic Controls

	Baseline	5-Year Follow-Up	Controls
Age, yrs	60 ± 7	64 ± 8	63 ± 9
Complications and comorbidities			
Hypertension	20 (39)	20 (39)	8 (40)
AMI	0 (0)	5 (10)	-
Dyslipidemia	26 (51)	22 (44)	10 (50)
Diabetic nephropathy	0 (0)	1 (2)	-
Diabetic retinopathy	0 (0)	7 (15)	-
Diabetic neuropathy	0 (0)	7 (15)	-
Hypogonadotropic hypogonadism	0 (0)	9 (18)	-
Hypergonadotropic hypogonadism	0 (0)	3 (6)	-
Subclinical hypogonadism	2 (4)	15 (29)	-
Erectile dysfunction	15 (29)	18(35)	-
Treatment			
Metformin	27 (53)	34 (67)	-
Secretagogues	14 (27)	10 (20)	-
Insulin	0 (0)	2 (5)	-
Liraglutide	0 (0)	4 (8)	-
Statin	14 (27)	28 (55)	10 (50)
ACE inhibitor	8 (16)	16 (31)	6 (30)
AT1-blocker	13 (25)	15 (29)	5 (25)
Calcium-channel blocker	7 (14)	12 (24)	4 (20)
β-blocker	5 (10)	8 (16)	2 (10)
AT1-blocker + diuretic	4 (9)	9 (18)	4 (20)
Diuretic	3 (6)	16 (31)	6 (30)

Values are mean ± SD or n (%).

ACE = angiotensin=converting enzyme; AMI = acute myocardial infarction; AT1 = angiotensin 1; CMR = cardiac magnetic resonance; T2DM = type 2 diabetes mellitus.

reconstruction for recurvatum penile surgery. After seeding, only sprouting cells were used for subcultivation. Cells at low passages were used for experiments. Cells were maintained throughout in Dulbecco's Modified Eagle Medium (DMEM) low glucose (1 g/l) or high glucose (25 mmol/l, 4.5 g/l) supplemented with 10% Fetal Bovine Serum (Life Technologies, California) 2 mmol/l L-glutamine, 1 U/ml penicillin, and 1 μg/ml streptomycin solution (Sigma Aldrich, Missouri), as shown (13). HL-1 and human pericytes were stimulated with 2 ng/ml recombinant transforming growth factor β1 (Peprotech, London, United Kingdom) for 48 h.

miRNA TRANSFECTION AND 3'UTR LUCIFERASE ASSAY. In this study, 10^5 cells were seeded in triplicate in 12-well plates and allowed to settle for 16 h and then transfected with Lipofectamine 3000 (Life Technologies, California) according to the manufacturer's instructions. The cells were cotransfected with 250 ng of pISImmP16 3' UTR (Addgene, Massachusetts) or MMP2 3' UTR plasmid, kindly provided by Dr. Giovanna Castoldi (Bicocca University, Monza, Italy), with or without 10 nmol/l of miR122-5p, miR595 (Sigma Aldrich, California), or miR499 (Origine, Massachusetts). Firefly luciferase activity was measured 24 h after transfection with the Dual-Luciferase Reporter Assay System (Promega, Mannheim, Germany) using a GloMax 96 Microplate Luminometer (Promega) according to the manufacturer's instructions.

REAL-TIME PCR ANALYSIS. For miRNA real-time PCR and tissue gene expression analyses see Methods 6 in Supplemental Appendix.

METALLOPROTEINASE GELATIN ZYMOGRAPHY. The medium was collected 48 h after transfection and gelatinase (matrix metalloproteinases [MMP] type 2 and 9) activity was visualized using zymography. The medium was separated under nonreducing conditions in a 12% Sodium Dodecyl Sulphate - Poly-Acrylamide Gel Electrophoresis (SDS-PAGE) solution containing 10 mg/ml gelatin. After electrophoresis, the gels were incubated with 2% Triton X-100 (twice for 60 min) to remove Sodium Dodecyl Sulphate (SDS) incubated overnight at 37°C in buffer containing 50 mmol/l Tris-HCl (pH 7.5), 10 mmol/l $CaCl_2$, 100 mmol/l NaCl, and 2% Triton X-100. Gels were stained in 0.25% Coomassie blue for 1 h and destained until bands of activity were clearly visible. Gels were acquired with the Syngene G-box system (Syngene Bioimaging, Haryana, India) and MMP-2 and MMP-9 bands were quantitatively analyzed using ImageJ Software (National Institutes of Health, Bethesda, Maryland).

STATISTICAL ANALYSIS. Continuous variables are reported as mean ± SD. All variables were tested for normality using the Shapiro-Wilk test. Pearson test was performed to evaluate the potential correlation between clinical variables and miRNA levels. A 2-step analytic approach was used to test possible differences between cardiac dynamics parameters throughout the study timeframe: the first step consisted of nonlinear regression analyses with dynamic fit to compute individual cardiac dynamics' coefficients, and the second step consisted of pairwise (pre-post) comparisons using Student's *t*-test. The approach was selected for consistency with the published CECSID trial (5) and because individual coefficients can be used for subsequent follow-up evaluations. Regarding the other outcome measures, independent and pairwise comparisons were performed using Student's *t*-test and one way-analysis of variance, and linear regression models were used to explore dependency (SPSS for Windows, version 18.0, IBM). Data from in vitro experiments are presented as the mean ± SE of the mean from at least 3 separate experiments. Data significance was analyzed using Student's *t*-test for parametric data or Mann-Whitney

test for nonparametric data. A $p < 0.05$ was considered statistically significant.

RESULTS

CLINICAL CHARACTERISTICS OF THE STUDY POPULATION. A total of 79 men (age 64 ± 8 years) were enrolled, including 59 patients with T2DM who had completed the CECSID trial. Eight of these were lost to follow-up: 4 refused to undergo the last CMR examination, 1 died due to colorectal carcinoma, and 3 were excluded for symptomatic ischemic heart disease, no longer matching the inclusion criteria. The full dataset was, therefore, available for 71 subjects, 51 individuals with T2DM, and 20 controls (**Table 1**). Metabolic and anthropometric parameters remained unchanged throughout the study time (**Table 2** and Results 9.1 in Supplemental Appendix and Supplemental Table 1). All patients with diabetes and no control subjects showed baseline (5) and follow-up CMR-tagged imaging features consistent with diabetic cardiomyopathy (Supplemental Table 2). Post-hoc analysis revealed that 5 patients with diabetes (9.8%) showed focal subendocardial LGE areas consistent with asymptomatic ischemic damage, despite no 2-dimensional echo hypokinetic areas; these subjects were excluded in the subgroup analysis (Results 9.1 in Supplemental Appendix).

CMR GEOMETRY, KINETICS, AND PERFORMANCE: LONGITUDINAL ANALYSIS. Analysis of cardiac geometry showed an increase in LVMi, shaping a further progression of LV hypertrophic degree with an estimated increase of 3.37 ± 7.41 g/m^2/year individual variation in baseline mass. A borderline increase in EDVi ($p = 0.056$) was also observed.

Analysis of torsion and strain revealed worsening of strain, but no change in torsion (**Table 3**).

Analysis of contraction dynamics revealed a reduced TtP and RR. Similarly, there was a decrease in the systolic (T_{max}) and diastolic (T_o) torsion coefficient with an increase in twist time constant (b_t), but no change in recoil time constant (b_{ut}). EF (**Table 3**) and metabolic status (Results 9.2 in Supplemental Appendix) remain unchanged. For cross-sectional and longitudinal correlations see Results 9.3 in Supplemental Appendix.

SUBGROUP ANALYSIS. Although patients with acute symptomatic coronary syndrome were excluded during follow-up, post hoc CMR analysis revealed that 5 additional patients presented focal areas of LGE consistent with myocardial scar, not previously detected as electrocardiogram abnormalities or 2-dimensional echo ventricular contraction defects. All analyses were repeated excluding these subjects (Results 9.2 in Supplemental Appendix). In short, cardiac geometry analysis proved the significant progression of LV hypertrophy, but the unchanged EDVi suggests that dilation is probably associated with the ischemic damage, whereas hypertrophy might also develop independently. As with the whole cohort, impaired strain and unaffected torsion were observed, whereas EF remained unchanged. Subgroup analysis for hypogonadism was not significant.

TABLE 2 Metabolic and Anthropometric Parameters

	Baseline	5-Year Follow-Up	Delta	p Value
Weight (kg)	81.59 ± 14.93	82.10 ± 15.19	0.52 ± 4.36	0.495
BMI (kg/m^2)	27.42 ± 4.50	27.28 ± 4.28	−0.04 ± 1.61	0.877
Waist circumference (cm)	99.45 ± 11.81	99.63 ± 13.04	0.18 ± 6.95	0.871
HbA1c (mmol/mol)	57.40 ± 11.42	55.10 ± 12.73	−2.10 ± 0.97	0.230
Total cholesterol (mmol/l)	5.45 ± 1.07	5.11 ± 1.95	-0.34 ± 1.29	0.139
LDL (mmol/l)	3.22 ± 1.12	2.81 ± 0.99	−0.42 ± 1.14*	0.048
HDL (mmol/l)	1.30 ± 0.31	1.40 ± 0.36	0.10 ± 0.03	0.091
Triglycerides (mmol/l)	1.38 ± 0.82	1.36 ± 0.64	−0.19 ± 0.89	0.906
Creatinine (μmol/l)	82.20 ± 14.21	79.91 ± 21.89	−2.28 ± 13.54	0.312
Microalbuminuria (mg/l)	14.65 ± 23.07	18.83 ± 34.79	3.38 ± 8.79	0.518

Values are mean ± SD. *$p < 0.05$.
BMI = body mass index; HDL = high-density lipoprotein; LDL = low-density lipoprotein.

miRNA ARRAY STUDY. Individual microarray analysis was performed using the common 2-steps biostatistics approach (10) (Methods 5 in Supplemental Appendix) on patient serum samples at baseline and follow-up to check for any longitudinal differential expression of circulating miRNAs. miR122-5p was confirmed as regulated (**Figure 1**) and selected as differentially expressed. Linear regression demonstrated that miR122-5p predicted RR ($\beta = -11.33$; 95% confidence interval [CI]: −20.43 to −2.24; $p = 0.03$). Target-scan and network analysis revealed that miR122-5p predicted the MMPs and their regulators (Tissue Inhibitor of Metalloproteinases-1) as converging targets.

To prove the involvement of miR-122-5p in diabetic cardiomyopathy, we first analyzed its tissue and cell expression. Then, we tested its up-regulation in the high-glucose settings. Finally, we explored the predicted targets documenting whether its up-regulation could suppress MMPs or modify their enzymatic activity, thus providing compelling evidence that miR-122-5p affects ECM remodeling.

miR122-5P EXPRESSION IS ASSOCIATED WITH DIABETIC CARDIOMYOPATHY IN VIVO. miR122-5p was once considered a tissue-specific miRNA because it is highly expressed in the liver. However, later studies investigated its role in HF (14). The predominant factor in diabetes-mediated complications is endothelial

TABLE 3 CMR Assessment of Dynamics and Geometric and Performance Parameters

	Baseline	5-Year Follow-up	Delta	p Value
Torsion, θ (°)	19.53 ± 4.41	19.28 ± 4.64	0.24 ± 4.04	0.737
Strain, σ (%)	−12.17 ± 2.76	−10.65 ± 3.15	1.52 ± 3.85†	0.033
Tmax	26.31 ± 6.07	19.04 ± 4.76	−7.27 ± 6.18*	0.000
b_t	0.22 ± 0.07	0.55 ± 0.22	0.33 ± 0.21*	0.000
TTP (ms)	160.19 ± 27.96	125.0 ± 25.0	−35.18 ± 28.81*	0.000
T_O	21.95 ± 5.37	15.32 ± 3.90	−6.63 ± 4.90*	0.000
b_{ut}	0.20 ± 0.07	0.15 ± 0.11	−0.04 ± 0.13	0.146
RR (s^{-1})	47.88 ± 17.28	27.87 ± 13.11	−20.01 ± 19.07*	0.000
LVMi (g/m^2)	118.52 ± 25.37	131.99 ± 27.27	13.47 ± 29.66†	0.014
EDVi (ml/m^2)	60.53 ± 15.06	65.70 ± 15.15	5.16 ± 14.71	0.056
CI (g/ml)	2.01 ± 0.44	1.97 ± 0.41	−0.03 ± 0.34	0.628
EF (%)	60.76 ± 9.02	60.76 ± 6.42	0.00 ± 8.31	0.998

Values are mean ± SD. *p < 0.0001. †p < 0.05.

b_t = torsion constant; b_{ut} = recoil constant; CI = concentricity index; EDVi = end-diastolic volume index; EF = ejection fraction; LVM = left ventricular mass index; RR = normalized recoil rate; T_{max} = torsion coefficient; T_O = decay coefficient; TTP = time to peak; other abbreviation as in Table 1.

dysfunction. T2DM causes amplification of endothelial cell dysfunction, glycosylation of ECM proteins, and vascular denervation, ultimately leading to impaired neovascularization and diabetic wound healing. MMPs are highly expressed by pericytes, local regulatory cells that are important for maintaining vascular homeostasis and hemostasis (15). miR122-5p expression analysis on the liver and the heart isolated from 5- and 22-week-old wild-type mice confirmed that miR122-5p is expressed and regulated in heart tissue (Figure 2A) and the endothelial cell compartment (Figure 2B).

miR122-5P DIRECTLY BINDS MMP-2 3'UTR AND MODULATES ECM GENE EXPRESSION. miR122-5p was predicted by TargetScan and miRanda analysis to bind the MMP-2 messenger RNA (mRNA) 3'UTR. To determine whether MMP-2 was regulated by miR122-5p, we cotransfected HEK293 cells with a wild-type construct (3'UTR-MMP-2) and an unrelated control miRNA (miR499) or with miR122-5p. There was a significant decrease in luciferase in cells overexpressing miR122-5p, suggesting that it directly binds the 3'UTR of MMP-2 (Figure 3A). Since we demonstrated that miR122-5p is mainly produced by the endothelial compartment, we evaluated MMP-2 modulation after miR122-5p overexpression in a human pericyte cell model. As reported in Figure 3B, miR122-5p reduced MMP-2 expression and increased the mRNA levels of various ECM markers.

HYPERGLYCEMIA EXACERBATES THE MMP-2 RELATED ECM REMODELING INDUCED BY miR122-5P. To resemble the diabetic milieu, pericytes were cultured in high-glucose conditions (25 mmol/l) and after 1 week the cells were transfected with miR122-5p or miR499 unrelated control. Real-Time-qPCR analysis showed reduced MMP-2 levels in miR122-5p overexpressing cells, whereas the ECM markers COL1A1, ITGβ1, and VINCULIN were increased (Figure 4A). MMP-2 down-regulation parallels the decreased activity of these cells, as demonstrated by zymography analysis on supernatant from miR122-5p overexpressing pericytes (Figure 4B). The high-glucose environment alone was sufficient to reduce MMP-2 activity (Figure 5A) and induce ECM remodeling (Figure 5B).

DISCUSSION

Our study provides the first description of longitudinal change in CMR features and circulating miRNAs in a homogeneous cohort of men with T2DM followed up to 5 years after diagnosis. Despite good glycemic control, we observed a tendency toward left ventricular chamber dilation accompanied by an upscaling of cardiac hypertrophic degree. The cardiac kinetics changed accordingly: torsion, increased at baseline, plateaued, thus failing to compensate for any further strain reduction observed at follow-up. The twisting and untwisting coefficients followed the progressive depletion of the spring mechanism, consistent with a deterioration of the viscoelastic myocardial properties, mirrored by miR122-5p up-regulation. In vitro studies demonstrated that miR122-5p down-regulates MMP-2, one of the enzymes responsible for ECM rearrangement in diabetes (16) (Central Illustration).

The clinical significance of the evolution of cardiac hypertrophy toward a "thick and dilated" phenotype lies in the 5% incidence of acute coronary syndrome and an additional 8% CMR findings of asymptomatic ischemic scars, all notwithstanding good metabolic control throughout the follow-up period.

New glucose-lowering drugs (GLP1-RA and SGLT2i) have been proven to improve cardiovascular events in patients with T2DM. However, they are regarded as second-line treatment and their efficacy appears more striking in secondary, rather than primary, prevention (17). Moreover, most of the patients in our cohort were in good glycemic control not needing second-line treatments. Very few studies have longitudinally assessed the progression of cardiac remodeling in diabetes. In the large Olmsted County cohort study, 38.5% of patients with HFpEF evolved toward HFrEF during 5 years (18) through progressive contractile dysfunction or unique remodeling contributing to the pathophysiology of HFpEF. However, this cohort held the limit of observational studies and included a higher prevalence of HFpEF in

women (men and women may progress differently (19)), the evaluations were performed using conventional echocardiography, and the EF decrease was greater in those who were older and had coronary artery disease. In our prospective study on younger men studied with CMR, we did not find a decrease in EF during 5 years.

Significant advances have been made in understanding diabetic cardiomyopathy pathophysiology, but the role of glycemic control in accelerating or slowing cardiac remodeling is still unclear. Hyperglycemia is undoubtedly a major trigger for inflammatory/profibrotic pathways within the myocardium (20) as well as responsible for the progression toward HF, with an 8% increased risk for each 1% increase in HbA1c (21). Although metabolic parameters were unchanged in our cohort, and patients were in good control, heart disease progressed. This is consistent with previous observations showing that except in the very early

FIGURE 1 Circulating miRNA Regulation in T2DM Patients

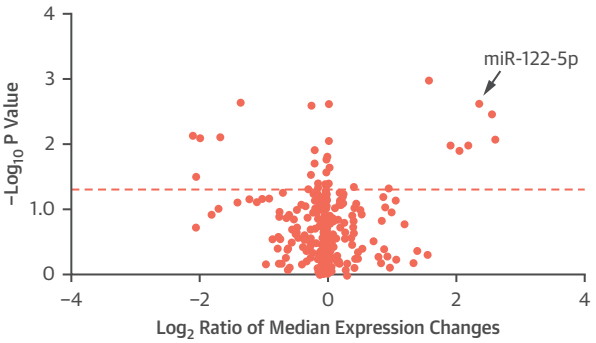

Volcano plot of microarray analysis. **(Arrow)** miRNA 122-5p. Y-axis: -Log_{10} p value (statistical difference in the variance between the baseline and the 5-yr follow-up); and X-axis: Log_2 of median expression changes between the baseline and the 5-yr follow-up.

FIGURE 2 miR-122-5p Expression Is Associated With Diabetic Cardiomyopathy In Vivo

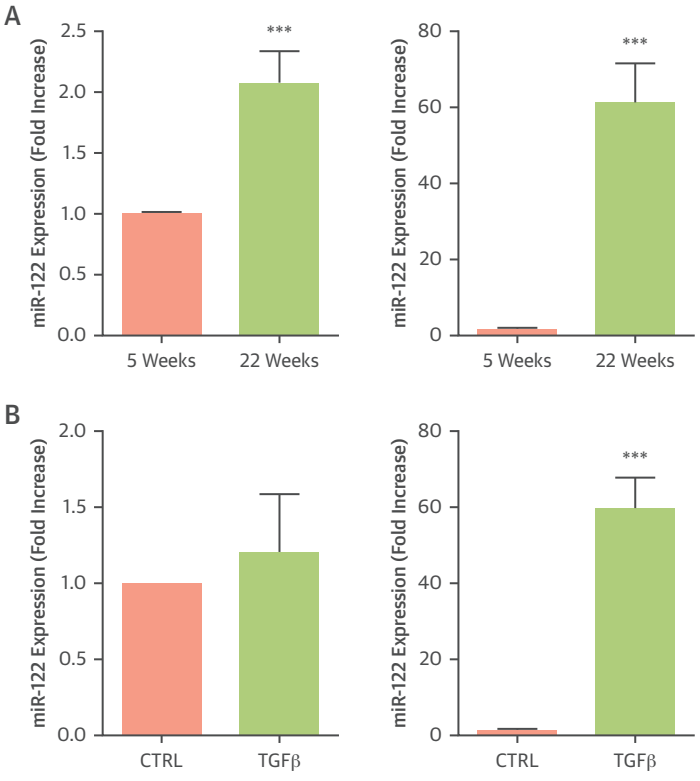

(A) miR-122 expression analysis using qPCR on liver **(left)** (n = 3) and heart **(right)** (n = 3) isolated from 5- and 22-week-old db/db mice. **(B)** miR-122 expression analysis using qPCR on TGFβ treated HL-1 **(left)** or human pericytes **(right)** (n = 3). Results are reported as mean ± SEM. ***p < 0.001. CTRL = controls; TGF = transforming growth factor.

FIGURE 3 miR-122-5p Directly Binds the MMP-2 mRNA 3′ UTR

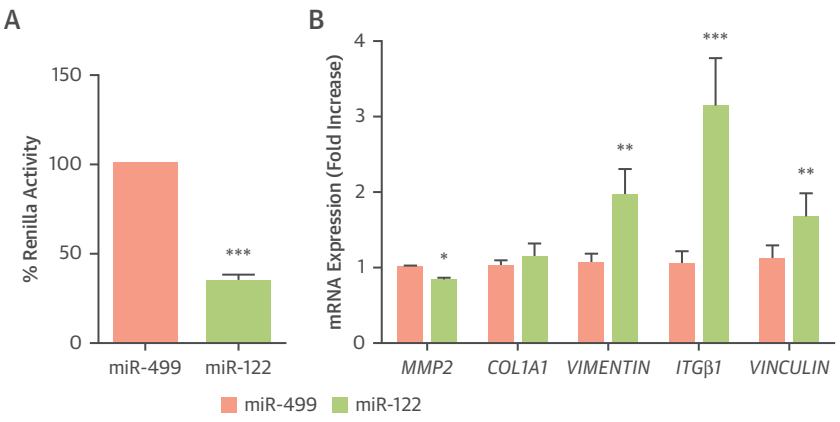

(A) Luciferase activity was measured on lysates of HEK293 cells cotransfected with MMP-2 3′ UTR and miR-122-5p or miR-499 (as unrelated control) (n = 3); **(B)** mRNA expression analysis of ECM markers by qPCR on human pericytes overexpressing miR-499 or miR-122-5p (n = 3). Results are reported as mean ± SEM. *p < 0.05; **p < 0.01; ***p < 0.001. COL1A1 = collagen type I alpha 1 chain; ECM = extracellular matrix; ITGb1 = integrin subunit beta 1; MMP = matrix metalloproteinase; mRNA = messenger RNA; other abbreviations as in Figure 2.

stage, strict glycemic control is insufficient to revert pathological cardiac processes (22).

Other important mediators are involved in the homeostasis of heart function. In recent years, miRNAs have been recognized as potential biomarkers for a wide spectrum of diseases, including T2DM (23). miR122-5p has been linked to T2DM and its complications (24) being also a prognostic biomarker for all-cause and cardiovascular mortality (25).

Our study observed at the 5-year follow-up a consistent up-regulation of miR122-5p in patients with CMR features of diabetic heart, confirming miR122-5p as a valuable biomarker to assess subclinical diastolic dysfunction (e.g., reduced RR) and earlier stages of diabetic cardiomyopathy (e.g., HFpEF) evolving toward dilated hypertrophy.

Target-scan and network analysis revealed converging evidence that the matrix proteins (namely MMP-2) could be a common target for miR122-5p. MMPs are a group of proteolytic enzymes involved in the ECM remodeling (26).

Through mechano-transduction, cardiac ECM regulates myocardial tension transmission in response to mechanical forces. Recent findings suggest the SGLT-2 mediated effects on mechanosensitive ion channels as potential pathways by which they act, improving diastolic dysfunction and cardiovascular risk in diabetic cardiomyopathy (27).

Also, imbalances in ECM processing by MMPs, specifically MMP-2 and MMP-9, have been associated with a wide spectrum of cardiovascular disorders, including diabetic cardiomyopathy (28), often with conflicting findings. Some of these inconsistencies are probably due to measuring their total serum levels, rather than assessing their tissue protease activity. However, even when measured through myocardial sampling approaches, the normal matrix architecture and balance between MMPs and tissue inhibitors of metalloproteinases could be affected by sample handling, thus not necessarily reflecting the dynamic nature of this proteolytic system (16). The transition from an apparently compensated remodeling to a failing heart depends on this equilibrium, which needs to be quantified promptly, using sensitive approaches.

Consistent with previous data on experimental models of diabetic cardiomyopathy (29), our in vitro data showed that increased miR122-5p levels down-regulate MMP-2 activity. Interestingly, a longitudinal evaluation of 53 patients with T2DM found reduced MMP-2 tissue activity at 3 months of follow-up (30), supporting our findings.

In our previous study, we demonstrated that the early stage of diabetic cardiomyopathy involves increased ventricular torsion due to defective shortening in the more fragile subendocardial fibers (5). The systolic twist is an intrinsic movement of the healthy heart resulting from the helical orientations of the fibers. It facilitates uniform transmural fiber shortening and wall stress, thereby improving the efficiency of ventricular contraction. This functional geometry also accommodates fiber length changes at constant ventricular volume (isometric contraction and relaxation), which

FIGURE 4 **High-Glucose Exacerbates MMP-2-Related ECM Remodeling Induced by miR-122**

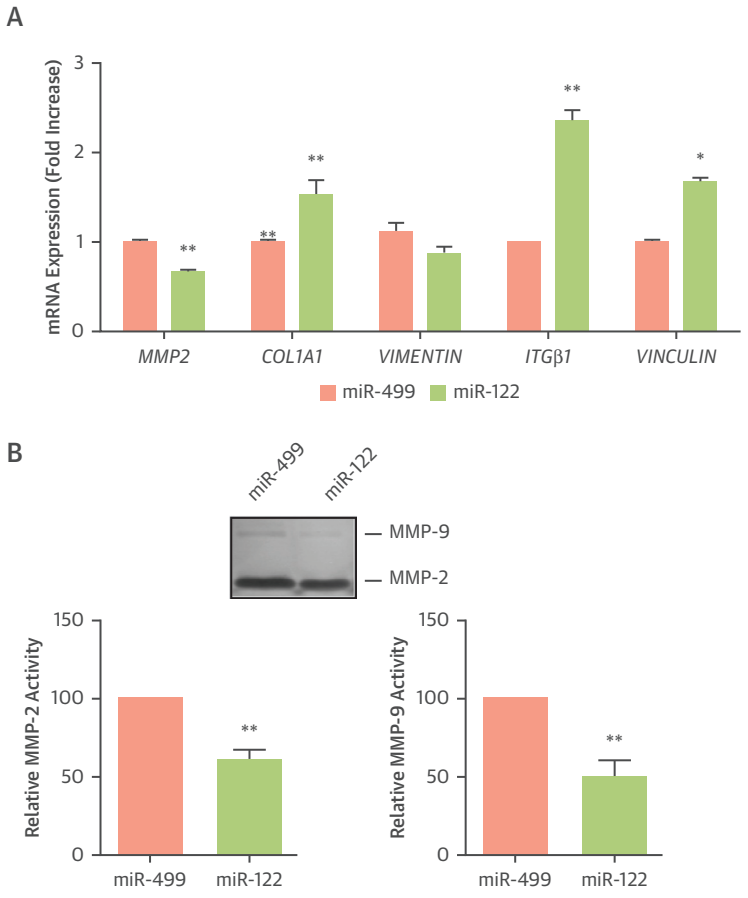

(A) mRNA expression analysis of ECM markers by qPCR on human pericytes overexpressing miR-499 or miR-122-5p conditioned by 1 week of high-glucose medium; **(B)** 48 h after transfection, media were collected and MMP-2 and MMP-9 activities were evaluated using zymography. Results are reported as mean ± SEM (n = 3). *p < 0.05; **p < 0.01. Abbreviations as in **Figures 2 and 3**.

improves ventricular ejection and filling. However, when torsion increases without a significant increase in shortening, in other words, when twisting is decoupled from strain, torsion becomes a form of dissipated energy. In diabetic cardiomyopathy, subendocardial fibrosis (5) causes torsion to rise and strain to decrease. The damage this triggers is initially limited to the thinner and shorter subendocardial fibers, which are orthogonal to the subepicardial fibers; this leads to increased torsion of the subepicardial fibers because it is no longer antagonized. The torsion measured by CMR comprises the absolute difference in these forces (31) (Supplemental Figure 1).

Our long-term follow-up showed that the already increased torsion did not progress further. In fact, the maximum torsion angle progressively diminishes when many cardiac fibers have undergone fibrotic changes (32), but only after extensive remodeling has already occurred (e.g., increased EDV) (33). At baseline, our patients had a low-normal EDVi and increased torsion. Five years later, they presented increased EDVi and unchanged torsion with reduced shortening, confirming the depletion of the compensatory mechanism described. The progressive increase in LVMi depicts an evolution toward "both thick and dilated hypertrophy" (34) (**Central Illustration**).

As previously mentioned, the description of the stages of diabetic cardiomyopathy has changed over time. Two types of remodeling (restrictive or dilated diabetic cardiomyopathy) have been described, only partially overlapping with HFpEF and HfrEF definitions, and the transition from restrictive to dilated

FIGURE 5 High Glucose is Sufficient to Induce MMP Reduction and ECM Remodeling

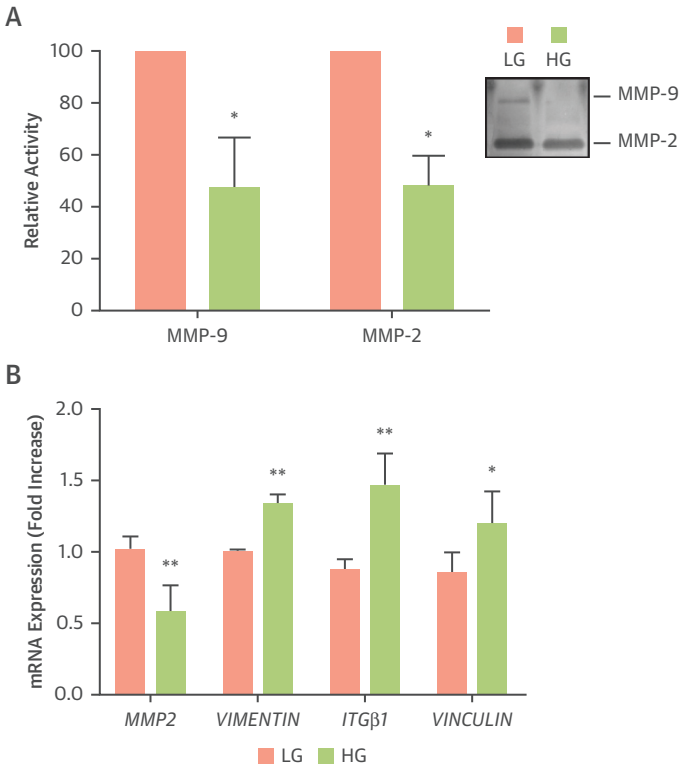

(A) Supernatants from human pericytes conditioned by 1 week of high-glucose or low-glucose media were collected and MMP-2 and MMP-9 activities were evaluated using zymography. Results are reported as mean ± SEM (n = 3); **(B)** mRNA expression analysis of ECM markers using qPCR on human pericytes conditioned by 1 week of high-glucose or low-glucose media. Data are reported as mean ± SEM (N = 3). *p < 0.05; **p < 0.01. HG = high-glucose; LG = low-glucose; other abbreviations as in Figures 2 and 3.

diabetic cardiomyopathy is considered "unlikely" (35) because each phenotype has specific underlying mechanisms (36). In restrictive diabetic cardiomyopathy, concentric LV remodeling is caused by coronary microvascular endothelial inflammation. A second hit (often ischemic) is needed for evolution to dilated eccentric LV remodeling, which involves loss of EF with concomitant cardiomyocyte cell death (37). Our data are consistent with this concept. The impaired diastolic function found at baseline reflects subclinical impaired contractility, not yet measurable through a reduced EF. Furthermore, as confirmed by the subgroup analysis, dilation was a hallmark of silent ischemic damage.

To investigate whether the observed alterations were intrinsic to the myocardium, we investigated the dynamics of cardiac contraction (twist) and relaxation (untwist or recoil). As in a spring, during twist potential energy is accumulated by the myocardial fiber (and ECM) and returned in the form of kinetic energy (about 40%) in the early untwist (38). Cardiac remodeling in diabetic cardiomyopathy reduces the potential energy stored during the systolic phase (39).

Our data revealed these changes in the heart's viscoelastic properties: less energy is accumulated because contraction meets lower resistance in reaching maximum torsion (39). Thus, the systole is shorter (reduced TTP) and less effective (reduced strain), and energy is dissipated (increased b_t, lower asymptotic torsion, Tmax). The diastolic phase is also impaired by a slower recoil rate, resulting in a less effective suction. The reduced RR reflects the impaired early untwisting (isovolumic relaxation), as further confirmed by a significant decrease in T_o. The changes in contraction dynamics, consistent with changes in the viscoelastic properties of the tissue, strongly suggest that the cardiac ECM is involved. Although a larger prospective cohort confirmation is needed, our results suggested that impaired diastolic function is related to the changes in miR122-5p, which could be considered not just a marker, but intrinsically implicated in the progression of diabetic cardiomyopathy.

STUDY LIMITATIONS. First, it should be noted that CMR accuracy could be limited by focal microvascular ischemic myocardial injury. Our study has limited information about patients' microvascular coronary artery disease progression; however, a dedicated study cannot be performed as none of the patients had clinical indication to coronary angiography according to current international guidelines (40). It is, therefore, important to acknowledge the lack of information about the microcirculation and progression of coronary artery disease.

Second, T1-mapping analysis would have helped to investigate interstitial fibrosis better. Although this is our current approach in ongoing studies (NCT01803828), at the time this study was designed, this technique was not yet routinely available. Third, only men were recruited. This is an advantage for homogeneity of the data, but obviously, the findings cannot be extrapolated to women. Finally, a larger cohort is needed to validate the observed outcomes.

CONCLUSIONS

This study provides a long-term CMR assessment of the evolution of cardiomyopathy in middle-aged men with T2DM, demonstrating a gradual progression of morpho-functional cardiac remodeling, despite good

CENTRAL ILLUSTRATION Cardiac Contraction

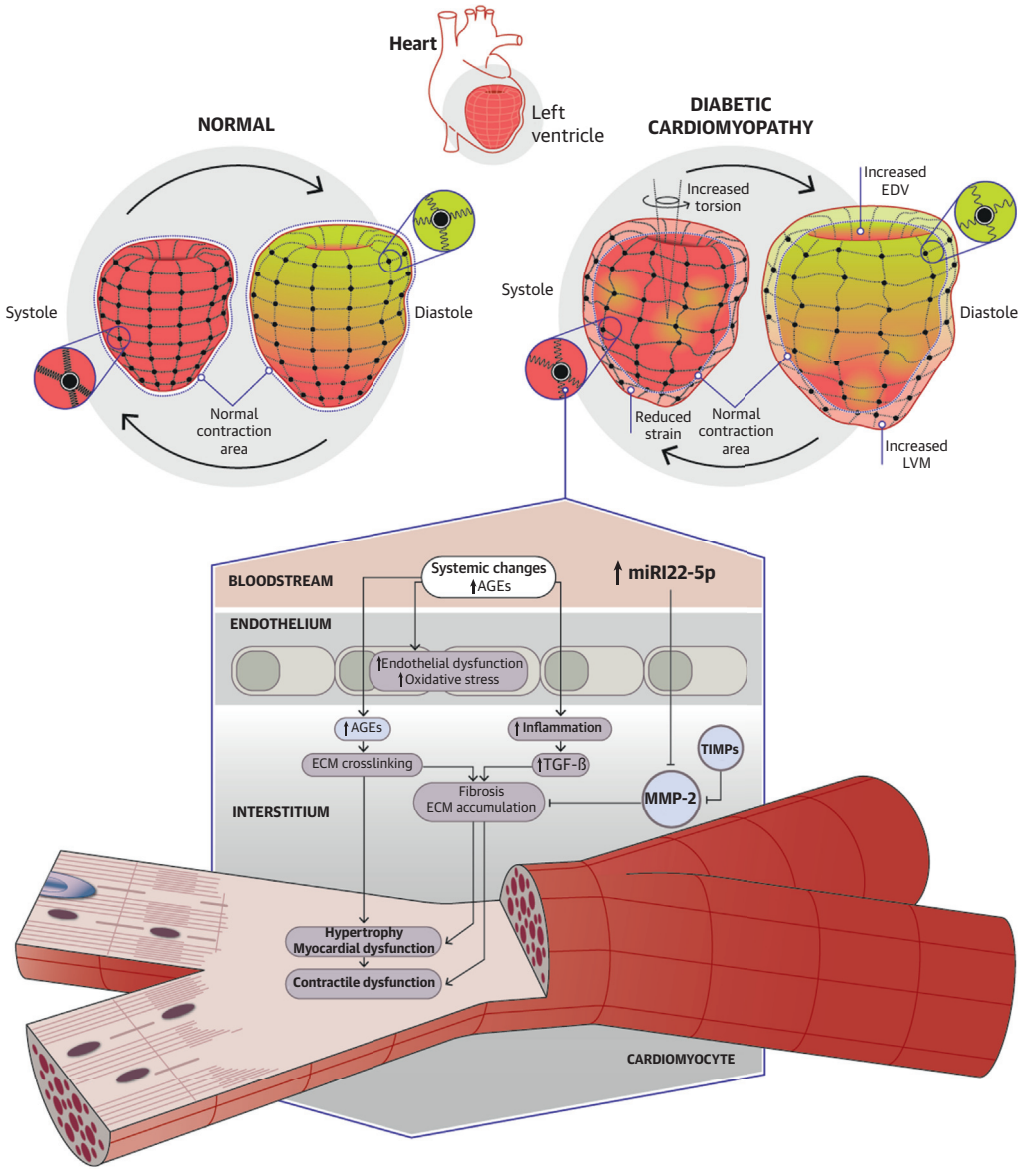

Pofi, R. et al. J Am Coll Cardiol Img. 2020;■(■):■-■.

Cardiac contraction in normal heart **(left)** and diabetic heart **(right)**. **(Bottom)** Proposed mechanisms underlying the kinetics abnormalities. AGE = advanced glycation end-product; ECM = extracellular matrix; EDV = end diastolic volume; LVM = left ventricular mass; MMP = matrix metalloproteinase; TGF = transforming growth factor; TIMP = tissue inhibitors of metalloproteinase.

glycemic control, over a 5-year span. Increased torsion is the hallmark of early stages, but rapidly reaches a plateau and exhausts its compensatory role. Ventricular mass increases with time, and the ventricular chamber tends to enlarge. The torsion eventually decouples from strain, which is persistently reduced throughout all stages of diabetic cardiomyopathy. The viscoelastic properties of the myocardium worsen, consistent with profibrotic or myofilament damage: the twist phase is shorter and less effective, and the untwist is loose. The heart seems to progress toward dilated hypertrophy, the stage immediately before HF, for which current treatments are largely ineffective. The ECM may be

involved in this and is a potential new target. CMR with miRNA analysis may be the only useful tools to assess such subclinical changes and follow the diabetic heart because remodeling does not seem sensitive to strict metabolic control. In conclusion, greater efforts should be made to understand the molecular mechanism underlying diabetic cardiomyopathy, and current treatments should be optimized to prevent and reverse the "natural" progression toward HF in patients with T2DM.

ACKNOWLEDGMENT Medical writing assistance was provided by Marie-Hélène Hayles during the preparation of the manuscript.

AUTHOR DISCLOSURES

The work was funded by the Italian Ministry of University and Research MIUR - PRIN 2015ZTT5KB. Dr. Isidori has received consultation fees, unconditional grants, and hospitality to conferences from IBSA, Takeda, and IPSEN. Dr. Filardi received hospitality to conferences from Sanofi and Merck. All other authors have reported that they have no relationships relevant to the contents of this paper to disclose.

ADDRESS FOR CORRESPONDENCE: Dr. Andrea M. Isidori, Department of Experimental Medicine, Sapienza University of Rome, Viale del Policlinico 155, 00161 Rome, Italy. E-mail: andrea.isidori@uniroma1.it. Twitter: @Groupisidori.

PERSPECTIVES

COMPETENCY IN MEDICAL KNOWLEDGE: Cardiovascular complications are the main causes of morbidity and mortality in patients with T2DM, accounting for about two thirds of overall deaths. The existence of a specific diabetic cardiomyopathy is supported by the 2- to 5-fold increase in HF in people with diabetes, even when adjusted for other most common risk factors. This further confirms diabetes as an independent cardiovascular risk factor. The mechanism of diabetic cardiomyopathy progression outside of major adverse cardiac event is still highly debated, as is the ability of strict glycemic control to halt or reverse such changes. Understanding the molecular mechanisms involved could help prevent its evolution into the fibrotic stage. Although novel drugs appear promising in secondary prevention, primary prevention of diabetic cardiomyopathy remains an unmet need. Physicians should be aware that, notwithstanding good glycemic control, 5% of patients enrolled experienced acute coronary syndrome and an additional 8% had CMR findings of asymptomatic ischemic scars throughout the follow-up period. The lesson derived from this long observational analysis is that cardiac remodeling continues, asymptomatically, involving a different compartment of the cardiac structure and a change in its physical properties. This underlines that current first-line treatments are largely ineffective against cardiac remodeling in diabetes and there is an urgent need for noninvasive biomarkers offering diagnostic, prognostic, and therapeutic targets that could also be used to follow the diabetic heart.

TRANSLATIONAL OUTLOOK: In this context of subclinical and asymptomatic cardiac damage, the widely used conventional echocardiography could not be sensitive enough to measure underlying subclinical cardiac morpho-functional changes triggered by diabetes mellitus and progressing despite glycemic control. CMR with tagging and more thoughtful analysis of contraction dynamics can disclose a wealth of asymptomatic changes occurring in diabetic cardiomyopathy. More morpho-functional studies, rather than simply morphological studies, are needed to follow-up patients with T2DM, merging imaging data with the search for novel biomarkers. Clinicians should reconsider cardiac performance as resulting from both contraction dynamics and elastic properties. In this context, asymptomatic diastolic dysfunction is one of the first signs of impaired elastic properties, which could be independent of the ischemic damage. We provided evidence that miRNAs, specifically the mIR122-5p, could represent a novel noninvasive approach to study diastolic dysfunction due to ECM remodeling, with the potential to offer diagnostic, prognostic, and therapeutic targets in diabetic cardiomyopathy progression.

REFERENCES

1. Grundy SM, Benjamin IJ, Burke GL, et al. Diabetes and cardiovascular disease: a statement for healthcare professionals from the American Heart Association. Circulation 1999;100:1134–46.

2. Kannel WB, Hjortland M, Castelli WP. Role of diabetes in congestive heart failure: the Framingham study. Am J Cardiol 1974;34:29–34.

3. Falcao-Pires I, Leite-Moreira AF. Diabetic cardiomyopathy: understanding the molecular and cellular basis to progress in diagnosis and treatment. Heart Fail Rev 2012;17:325–44.

4. Maisch B, Alter P, Pankuweit S. Diabetic cardiomyopathy-fact or fiction? Herz 2011;36:102–15.

5. Giannetta E, Isidori AM, Galea N, et al. Chronic Inhibition of cGMP phosphodiesterase 5A improves diabetic cardiomyopathy: a randomized, controlled clinical trial using magnetic resonance imaging with myocardial tagging. Circulation 2012;125:2323–33.

6. Jarnert C, Landstedt-Hallin L, Malmberg K, et al. A randomized trial of the impact of strict glycaemic control on myocardial diastolic function and perfusion reserve: a report from the DADD (Diabetes mellitus And Diastolic Dysfunction) study. Eur J Heart Fail 2009;11:39–47.

7. Colpaert RMW, Calore M. MicroRNAs in cardiac diseases. Cells 2019;8:737.

8. Cortez-Dias N, Costa MC, Carrilho-Ferreira P, et al. Circulating miR-122-5p/miR-133b ratio is a specific early prognostic biomarker in acute myocardial infarction. Circ J 2016;80:2183–91.

9. Li X, Yang Y, Wang L, et al. Plasma miR-122 and miR-3149 potentially novel biomarkers for acute coronary syndrome. PLoS One 2015;10:e0125430.

10. Fiore D, Gianfrilli D, Cardarelli S, et al. Chronic phosphodiesterase type 5 inhibition has beneficial effects on subcutaneous adipose tissue plasticity in type 2 diabetic mice. J Cell Physiol 2018;233:8411–7.

11. Venneri MA, Barbagallo F, Fiore D, et al. PDE5 Inhibition stimulates Tie2-expressing monocytes and angiopoietin-1 restoring angiogenic homeostasis in diabetes. J Clin Endocrinol Metab 2019;104:2623–36.

12. Campolo F, Zevini A, Cardarelli S, et al. Identification of murine phosphodiesterase 5A isoforms and their functional characterization in HL-1 cardiac cell line. J Cell Physiol 2018;233:325–37.

13. Park SW, Yun JH, Kim JH, Kim KW, Cho CH, Kim JH. Angiopoietin 2 induces pericyte apoptosis via alpha3beta1 integrin signaling in diabetic retinopathy. Diabetes 2014;63:3057–68.

14. Ali SKC, Abid M, Ahmad N, Sharma US, Khan NA. Pathological microRNAs in acute cardiovascular diseases and microRNA therapeutics. J Acute Dis 2016;5:9–15.

15. Amato B, Coretti G, Compagna R, et al. Role of matrix metalloproteinases in non-healing venous ulcers. Int Wound J 2015;12:641–5.

16. Spinale FG. Myocardial matrix remodeling and the matrix metalloproteinases: influence on cardiac form and function. Physiol Rev 2007;87:1285–342.

17. Zelniker TA, Wiviott SD, Raz I, et al. Comparison of the effects of glucagon-like peptide receptor agonists and sodium-glucose cotransporter 2 inhibitors for prevention of major adverse cardiovascular and renal outcomes in type 2 diabetes mellitus. Circulation 2019;139:2022–31.

18. Dunlay SM, Roger VL, Weston SA, Jiang R, Redfield MM. Longitudinal changes in ejection fraction in heart failure patients with preserved and reduced ejection fraction. Circ Heart Fail 2012;5:720–6.

19. Regensteiner JG, Golden S, Huebschmann AG, et al. Sex differences in the cardiovascular consequences of diabetes mellitus: a scientific statement from the American Heart Association. Circulation 2015;132:2424–47.

20. Chatham JC, Seymour AM. Cardiac carbohydrate metabolism in Zucker diabetic fatty rats. Cardiovasc Res 2002;55:104–12.

21. Stratton IM, Adler AI, Neil HA, et al. Association of glycaemia with macrovascular and microvascular complications of type 2 diabetes (UKPDS 35): prospective observational study. BMJ 2000;321:405–12.

22. Boussageon R, Bejan-Angoulvant T, Saadatian-Elahi M, et al. Effect of intensive glucose lowering treatment on all cause mortality, cardiovascular death, and microvascular events in type 2 diabetes: meta-analysis of randomised controlled trials. BMJ 2011;343:d4169.

23. Guay C, Regazzi R. Circulating microRNAs as novel biomarkers for diabetes mellitus. Nat Rev Endocrinol 2013;9:513–21.

24. Regmi A, Liu G, Zhong X, et al. Evaluation of serum microRNAs in patients with diabetic kidney disease: a nested case-controlled study and bioinformatics analysis. Med Sci Monit 2019;25:1699–708.

25. Stojkovic S, Koller L, Sulzgruber P, et al. Liver-specific microRNA-122 as prognostic biomarker in patients with chronic systolic heart failure. Int J Cardiol 2020;303:80–5.

26. Klein T, Bischoff R. Physiology and pathophysiology of matrix metalloproteases. Amino Acids 2011;41:271–90.

27. Nikolajevic Starcevic J, Janic M, Sabovic M. Molecular mechanisms responsible for diastolic dysfunction in diabetes mellitus patients. Int J Mol Sci 2019;20:1197.

28. Tan Y, Zhang Z, Zheng C, Wintergerst KA, Keller BB, Cai L. Mechanisms of diabetic cardiomyopathy and potential therapeutic strategies: preclinical and clinical evidence. Nat Rev Cardiol 2020;17:585–607.

29. Van Linthout S, Seeland U, Riad A, et al. Reduced MMP-2 activity contributes to cardiac fibrosis in experimental diabetic cardiomyopathy. Basic Res Cardiol 2008;103:319–27.

30. Poteryaeva ON, Russkikh GS, Zubova AV, Gevorgyan MM, Usynin IF. Changes in activity of matrix metalloproteinases and serum concentrations of proinsulin and C-peptide depending on the compensation stage of type 2 diabetes mellitus. Bull Exp Biol Med 2018;164:730–3.

31. Tavakoli V, Sahba N. Assessment of subendocardial vs. subepicardial left ventricular twist using tagged MRI images. Cardiovasc Diagn Ther 2014;4:56–63.

32. D'Hooge J, Claus P, Separovic J. Alterations of systolic left ventricular twist after acute myocardial infarction. Am J Physiol Heart Circ Physiol 2002;283:H2733–4.

33. Jia G, DeMarco VG, Sowers JR. Insulin resistance and hyperinsulinaemia in diabetic cardiomyopathy. Nat Rev Endocrinol 2016;12:144–53.

34. Khouri MG, Peshock RM, Ayers CR, de Lemos JA, Drazner MH. A 4-tiered classification of left ventricular hypertrophy based on left ventricular geometry: the Dallas heart study. Circ Cardiovasc Imaging 2010;3:164–71.

35. Seferovic PM, Paulus WJ. Clinical diabetic cardiomyopathy: a two-faced disease with restrictive and dilated phenotypes. Eur Heart J 2015;36:1718–1727,1727a–c.

36. Paulus WJ, Dal Canto E. Distinct myocardial targets for diabetes therapy in heart failure with preserved or reduced ejection fraction. J Am Coll Cardiol HF 2018;6:1–7.

37. Paulus WJ, Tschope C. A novel paradigm for heart failure with preserved ejection fraction: comorbidities drive myocardial dysfunction and remodeling through coronary microvascular endothelial inflammation. J Am Coll Cardiol 2013;62:263–71.

38. Sengupta PP, Korinek J, Belohlavek M, et al. Left ventricular structure and function: basic science for cardiac imaging. J Am Coll Cardiol 2006;48:1988–2001.

39. Knudtson ML, Galbraith PD, Hildebrand KL, Tyberg JV, Beyar R. Dynamics of left ventricular apex rotation during angioplasty: a sensitive index of ischemic dysfunction. Circulation 1997;96:801–8.

40. Knuuti J, Wijns W, Saraste A, et al. 2019 ESC Guidelines for the diagnosis and management of chronic coronary syndromes. Eur Heart J 2020;41:407–77.

KEY WORDS cardiac hypertrophy, cardiac magnetic resonance, diabetes mellitus, heart failure with preserved ejection fraction, metalloproteinase

APPENDIX For a supplemental methods section, tables, and a figure, please see the online version of this paper.